Poly(vinyl alcohol)-clay and Poly(ethylene oxide)-clay Blends Prepared Using Water as Solvent

NOBUO OGATA, SUGIO KAWAKAGE, TAKASHI OGIHARA

Department of Materials Science and Engineering, Fukui University, 3-9-1 Bunkyo, Fukui 910, Japan

ABSTRACT: Montmorillonite (MON) was solvent-cast blended with poly(vinyl alcohol) (PVA) and poly(ethylene oxide) (PEO) using water as cosolvent. The structure and properties of the blend films have been investigated. From small- and wide-angle X-ray scattering measurements of the blends, the silicate layers of MON are found to be well dispersed individually in the PVA–MON blends, while the silicate layers in PEO–MON blends are found to exist in the form of a large clay tactoid. Furthermore, for both blends, it is found that the silicate layers are parallel to the film surface of the blends, and that preferred orientation of polymer crystallites is induced by the presence of MON. The effects of the MON content on the thermal behavior of the PVA– and PEO–MON blends have been studied with a differential scanning calorimeter. Furthermore, the effects of geometry of the silicate layers on dynamic behavior of the blends have been studied. © 1997 John Wiley & Sons, Inc. J Appl Polym Sci **66:** 573–581, 1997

Key words: montmorillonite; poly(vinyl alcohol); poly(ethylene oxide); intercalation; X-ray scattering; dynamic mechanical analysis

INTRODUCTION

Inorganic particles are widely used as reinforcement materials for polymers. Among these inorganic materials, special attention has been paid to clay in the field of nanocomposites because of its small particle size and intercalation properties.[1–7] Montmorillonite (MON) is a smectite-type clay and has a layer structure. In the previous article,[8–10] the organically modified MON (OMON) was produced using distearyldimethylammonium chloride, and this OMON was blended with poly(*l*-lactide) (PLLA), poly(ε-caprolactone)(PCL), and poly(ethylene oxide) (PEO) using chloroform as cosolvent. We have investigated the structure of the blends and found that the modified clay has a notable structure in these blends. That is, the silicate layers forming the clay are not dispersed individually in the blends but they seem to exist in the form of the clay tactoid consisting of some silicate layers. Furthermore, their surface planes lie almost parallel to the surface of the blend film, and the tactoids are stacked with insertion of crystalline lamellae of the polymers in the film thickness direction. The presence of the clay also induces preferred orientation of the crystallites.

In order to study the formation mechanism of such notable structures of the blends, we have tried to investigate the structure of the blends of the unmodified MON and polymers such as poly-(vinyl alcohol) (PVA) and poly(ethylene oxide) (PEO). MON has hydrophilic nature and can be well dispersed by water. Moreover, PVA and PEO are highly soluble in water. Therefore, we prepared two solvent-cast blends, namely PVA–MON and PEO–MON, by using water as cosolvent. The aim of this work is to investigate the
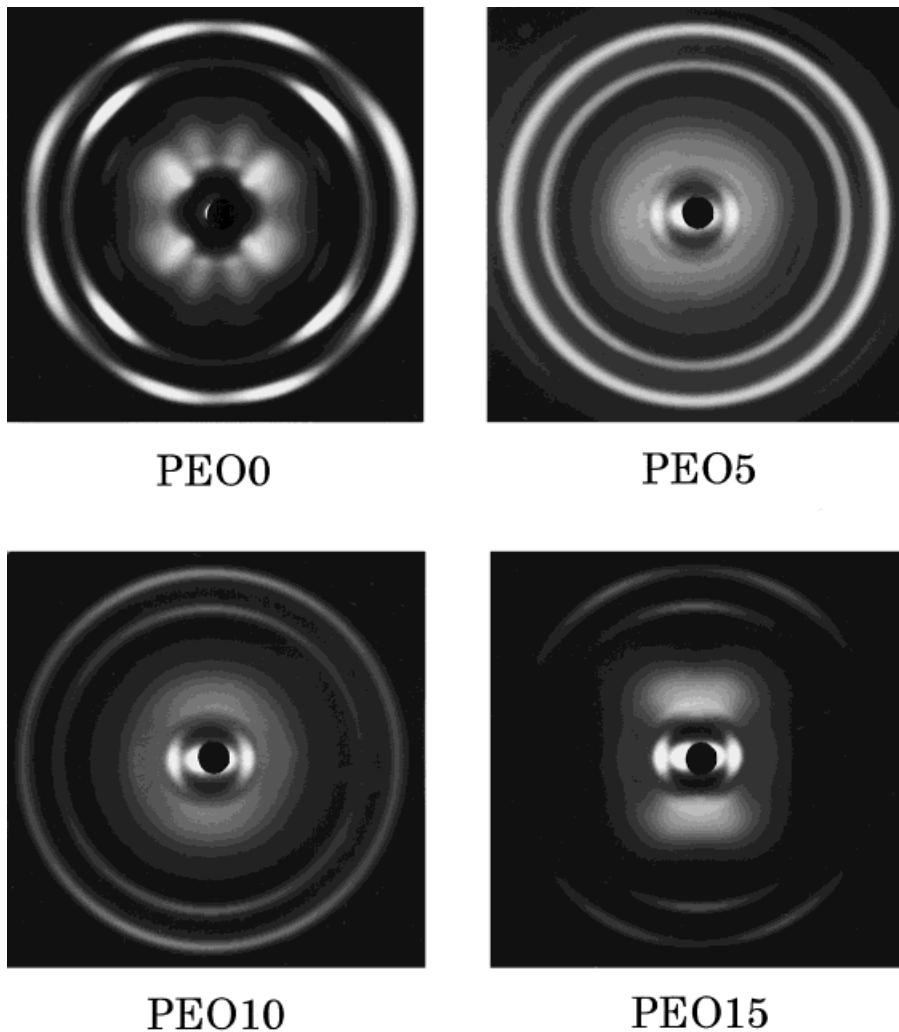
Figure 1 WAXS photographs of PEO–MON blends.

structure and properties of the two blends. Furthermore, the structure and mechanical properties of the PEO–MON are compared with those of the PEO–OMON blends; the structure and the properties of the PEO–OMON blends were reported in the previous article.[10]

EXPERIMENTAL

Materials

Montmorillonite "Kunipia F," (MON), was supplied by Kunimine Ind. Co. This clay has exchangeable sodium ions, and a cation exchange capacity of $\sim$ 120 mEq/100 g. PVA, with degree of polymerization (d_p) 1500, was purchased from WAKO Pure Chemical Industries Ltd; PEO, aver-

age molecular weight $(M_n) = 300,000$, was purchased from Aldrich Chemical Co.

Preparation of Blends

Given amounts of MON and powder PVA were placed in a Petri dish made of polystyrene; hot water was added and then the solution was kept at 50°C. After the water was vaporized, homogeneous films $\sim$ 0.1 mm thick were obtained. By using the same procedure, we also prepared the blend film of MON and PEO. The weight percentage of MON in the blend will be represented by the number followed by the abbreviated name of the polymers; for example, PVA10 indicates a PVA–MON blend containing 10 wt % of MON. MON will be also referred to as clay.
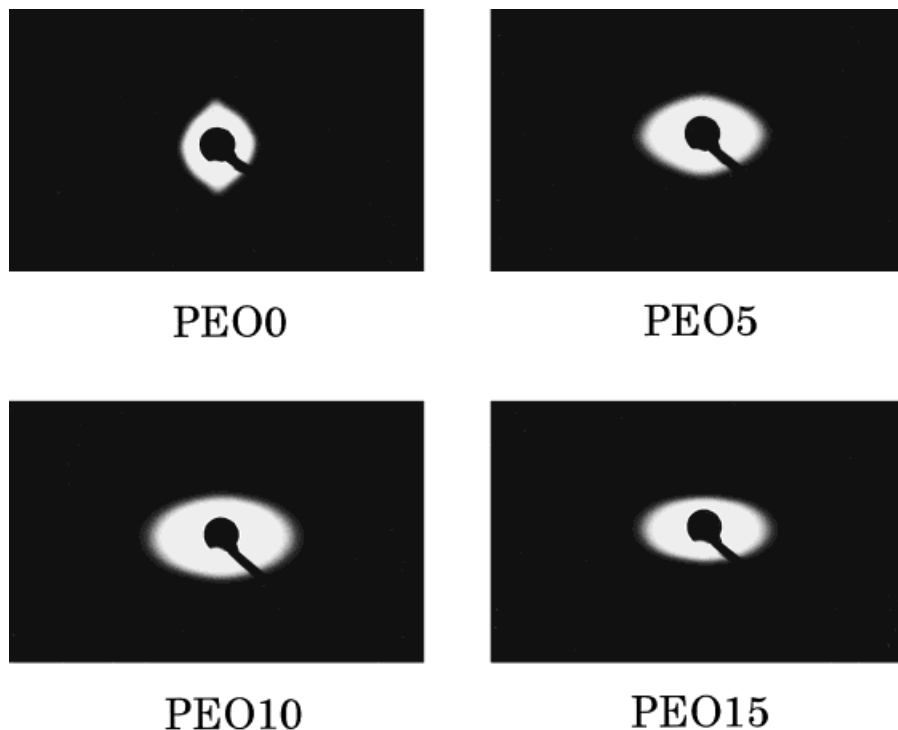
Figure 2 SAXS photographs of PEO–MON blends.

Characterization of Blends

Wide-angle X-ray scattering (WAXS) photographs were taken to the PEO–MON and PVA–MON blends with a flat camera having a pinhole slit, and with a Japan Electron Laboratory (JEOL, DX-GE-E) apparatus. Small-angle X-ray scattering (SAXS) photographs were also taken to the blends with a JEOL (JDX-8750) operated at 420 kV and 200 mA.

Thermal behavior of the blends was measured on a Perkin–Elmer DSC-7 (DSC) at a heating rate of 10°C/min under a nitrogen atmosphere. The melting point, T_m, and heat of fusion, ΔH_m, were evaluated from a maximum position of the endothermic peak and its area on the DSC curves, respectively.

Dynamic mechanical analyses (DMA) of the blends well dried with P_2O_5 were performed with a Rheometrics Scientific RSA II Viscoelastic Analyzer. Temperature scans at 1 Hz frequency were carried out with a heating rate of 2°C/min.

RESULTS AND DISCUSSION

Structure of Blends

The X-ray beam was incident on the blend films in through and edge directions, and WAXS and SAXS photographs were taken; the through and edge directions were perpendicular and parallel to the film surface, respectively. Since only the edge-view photographs showed characteristic patterns, we will show the view patterns in the following discussion. Figure 1 shows the WAXS photographs for the PEO–MON blends. The photographs of the blends show a pair of reflections on the equator near the beam stopper, while the photograph of PEO0 does not show such reflections. This means that the reflections originate in the presence of clay and the silicate layers of clay are stacked with periodicity, being parallel to the film surface; the reflections are derived from the (001) plane of clay.[11] It is noted that the reflection patterns originating in PEO crystallites change with the clay content. Preferred orientation of PEO crystallites can be clearly seen in PEO0. With increasing the clay content, preferred orientation disappears and an isotropic orientation pattern appears, and then preferred orientation reappears, as seen in PEO15. The same preferred orientation pattern seen in PEO15 was also observed in the PEO–OMON blends, which were solvent-cast blended using chloroform as cosolvent.[10] Moreover, a similar WAXS pattern was obtained from the sedimented mat of solution
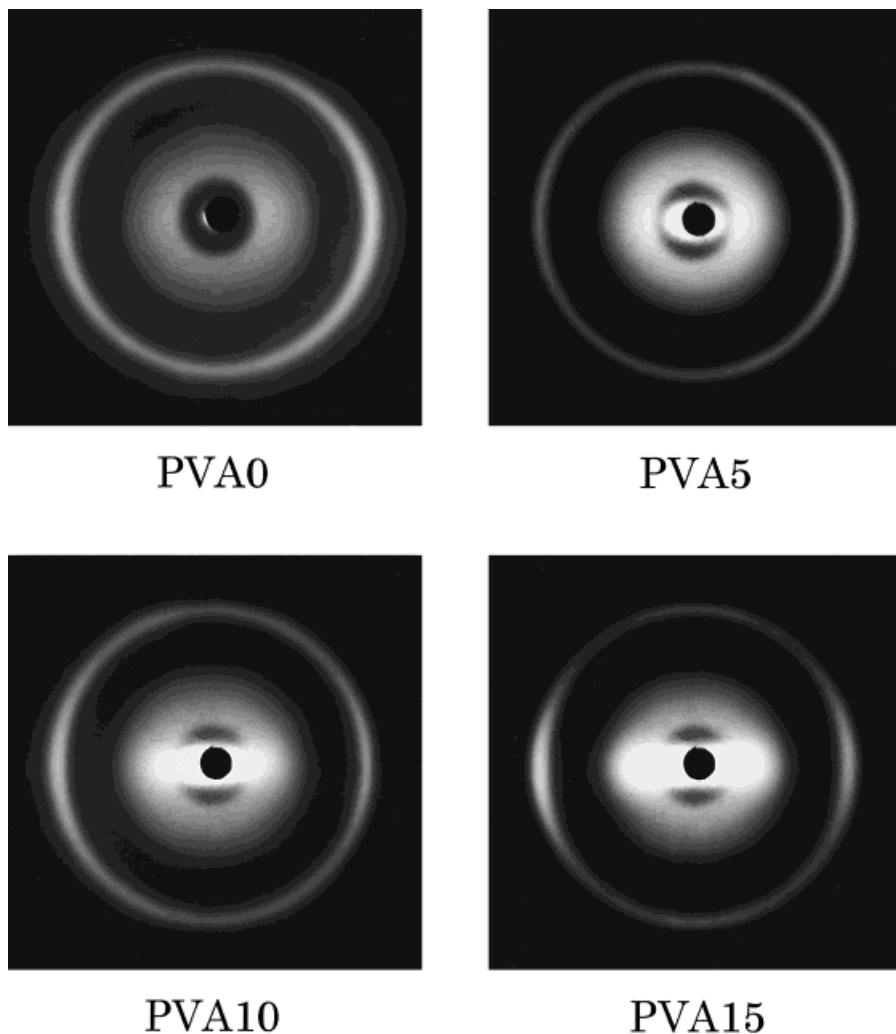
Figure 3 WAXS photographs of PVA–MON blends.

crystallized PEO single crystals when the X-ray beam was parallel to the mat plane.[12] From considering the WAXS pattern of the PEO mat and the results obtained here, we deduce that the chain direction of the PEO crystallites formed in the PEO15 is perpendicular to the surface of the silicate layers. The cast temperature used (50°C) was so high that preferred orientation of PEO crystallites would be induced under the influence of the clay. The appearance of preferred orientation means that the PEO crystallites are formed under the influence of the clay. In other words, the PEO crystallites are probably formed on the surface of the silicate layers. There is a large difference in the preferred orientation pattern between the PEO0 and PEO15 samples. By taking account of the WAXS pattern of the PEO mat, we

deduce that the chain axes of PEO0 tilt against the film surface with the angle $\sim \pm 45°$. In order to investigate the reason for preferred orientation seen in PEO0, we made also PEO0 samples in another three types of Petri dishes made of glass, Teflon, and stainless steel, using water as solvent. All the PEO0 samples more or less showed preferred orientation seen in PEO0 made in a polystyrene dish. This suggests that the solvent used, as well as the type of substrate, is an important factor in occurrence of preferred orientation, because the neat PEO sample cast with chloroform in a glass dish showed an isotropic orientation pattern. We cannot explain the mechanism for solvent and substrate influencing preferred orientation, much less the reason for the PEO crystallites showing the tilting angle $\pm 45°$, in this article.
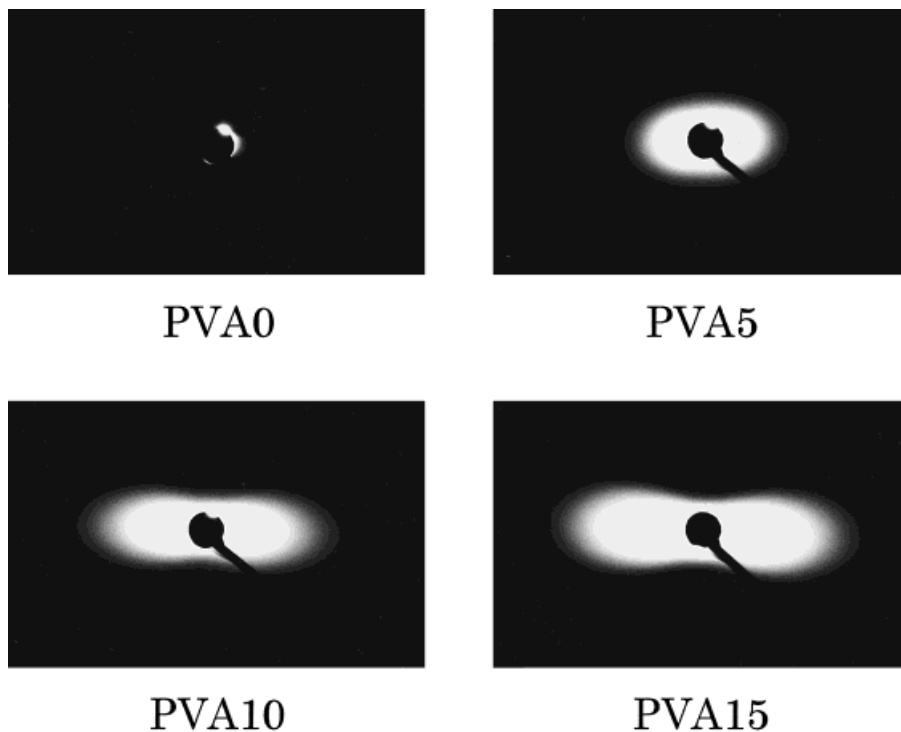
Figure 4   SAXS photographs of PVA–MON blends.

However, we can say at least that the PEO crystallites are formed under the influence of the clay in the blends.

Figure 2 shows the SAXS photographs for the PEO–MON blends. We can see a reflection around the beam stopper, but cannot see any periodicity originating from clay in the blends, despite the clay content. This result should be noted, because the PEO–OMON blends exhibited two pairs of reflections on the equator.[10] Apparently, the structure of MON formed in the PEO–MON blends is different from that of OMON formed in the PEO–OMON blends. Since SAXS patterns do not indicate any periodicity in PEO–MON blends, the size of the clay tactoids, consisting of silicate layers, seems to be markedly larger than that observed in the PEO–OMON blends. This reasoning is supported by the fact that MON cannot be well dispersed in PEO and the PEO–MON blends are brittle. Looking at the reasoning from a different angle, we can deduce that the organic modification reduces the size of the clay tactoids.

Figure 3 shows the WAXS photographs for the PVA–MON blends. A reflection ring originating in PVA crystallites can be seen. The intensity distribution does not seem to be uniform in the blends. That is, the reflection in the equatorial direction is stronger. By taking account of the pattern of drawn PVA fibers,[13] we deduce that the fiber axes of the PVA crystallites are parallel to the film surface. Furthermore, the photographs of the blends show a wide streak on the equator near the beam stopper, while the photograph of PVA0 does not show such reflection. Therefore, the streak originates in the presence of clay. Obscure periodicity can be seen on the equator of PVA10 and PVA15. It is noted that clear periodicity of the silicate layers, which is observed in PEO–MON blends (see Fig. 1), cannot be seen in PVA–MON blends. Figure 4 shows the SAXS photographs of the PVA–MON blends. We can see a reflection on the equator. The shape of the reflection changes with increasing the MON content (ϕ_{mon}). That is, a dumbbell-like reflection is developed with increasing ϕ_{mon}. Such type of reflection was observed in nylon 6-clay hybrids.[14] The ball-part of the reflection would be derived from periodicity of the clay tactoids. It should be noted that two pairs of reflections originating in the clay tactoids, which were observed in PLLA–OMON,[8] PCL–OMON,[9] and PEO–OMON[10] blends, cannot be seen in the PVA–MON blends. Therefore, periodicity of the tactoids seems to be relatively wrong in the PVA–MON blends. The WAXS and SAXS

patterns suggest that the silicate monolayers do not clearly form the clay tactoids, but are well dispersed individually in the blends, that is, delamination of the silicate layers occurs during the preparation of the PVA–MON blends. However, because a streak can be seen on the equator, the surface of the silicate monolayers seems to be almost parallel to that of the blend film. By considering the directions of the fiber axes of PVA crystallites and silicate layers, we can infer that the fiber axes of PVA crystallites are parallel to the silicate layers. This result should be noted because the fiber axes of PEO crystallites are perpendicular to the silicate surface, as described previously.

As discussed, although the same solvent, namely water, and the same unmodified MON were used for preparation of both PEO–MON and PVA–MON blends, the silicate layers and polymer crystallites seem to form different aggregations in the blends. This implies that the structure of the aggregations is strongly influenced by the chemical structure of polymers in the blends.

Thermal Behavior

Effects of the clay content on T_m and ΔH_m were investigated for the PEO–MON blends. The result is shown in Figure 5. A straight solid line was drawn through the values of ΔH_m at PEO0 and PEO100, where the value for ΔH_m at PEO100 was equal to zero. It can be seen that T_m decreases slightly with increasing the clay content (ϕ_{mon}).
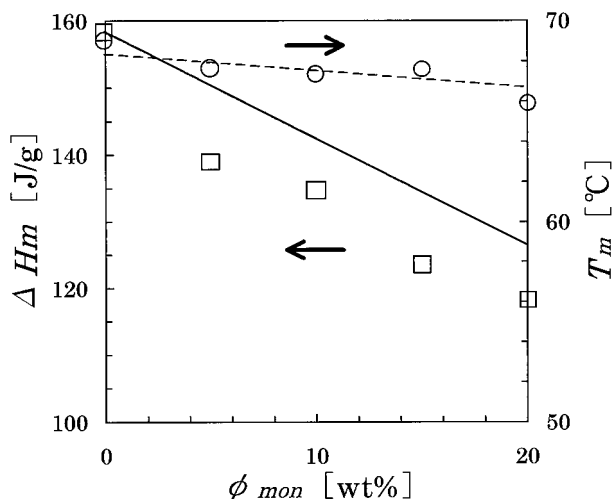

Figure 5 Effect of the MON content on T_m and ΔH_m of the PEO–MON blends.
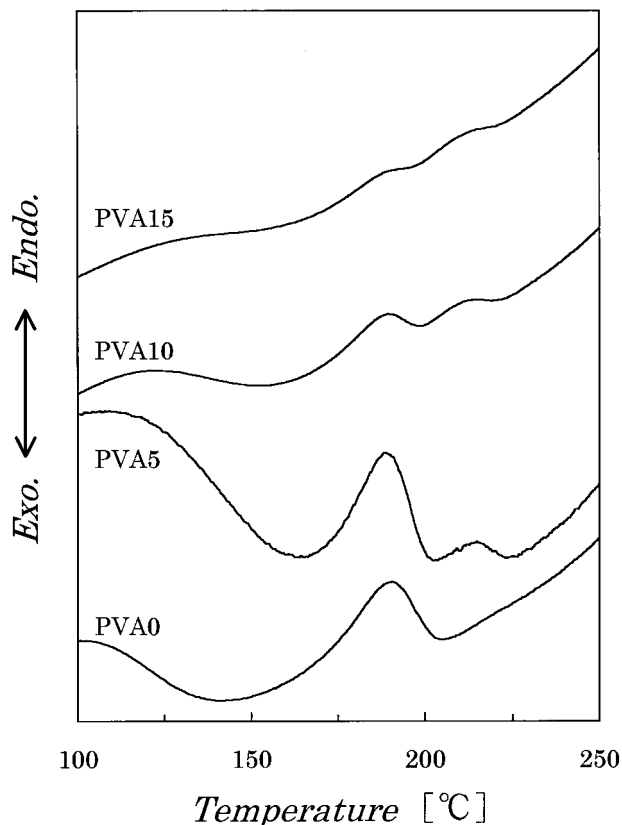

Figure 6 Effect of the MON content on the DSC curves of the PVA–MON blends.

This result implies that small-sized PEO crystallites are formed in the presence of the clay. It can be also seen that the experimental ΔH_m values are almost parallel to and under the straight line. This means that the total crystallinity of PEO is influenced by the presence of the clay. That is, the amorphous region of PEO increases with increasing ϕ_{mon}. In other words, intercalation of PEO molecules into the silicate layers may take place to some extent. However, because the spacing of the (001) plane of MON is not changed much by blending, intercalation does not seem to take place extensively.

Figure 6 shows the effect of the clay content on the DSC curves of the PVA–MON blends. An endothermic peak can be seen at ~ 190°C in the neat PVA0. On the other hand, the blend samples show two endothermic peaks; the peak at higher temperature develops with increasing ϕ_{mon}. The peak may correspond to the melting of the PVA crystallites that have a strong interaction with the clay. It is noted that these endothermic peaks become small with increasing ϕ_{mon}. Values for T_m
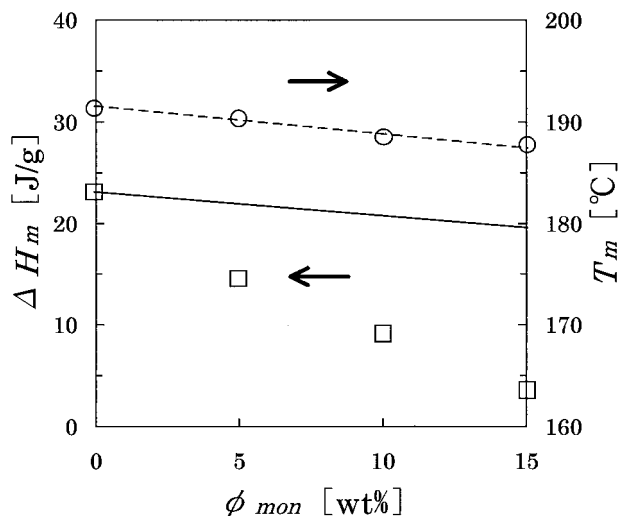
Figure 7   Effect of the MON content on the values for T_m and ΔH_m of the PVA–MON blends.

and ΔH_m evaluated from the low temperature peaks are plotted in Figure 7. By using the procedure explained previously (see Fig. 5), we draw a solid line for ΔH_m. It can be seen that T_m decreases and ΔH_m decreases markedly with increasing ϕ_{mon}. The deviation of the experimental ΔH_m value from the solid line is large for the PVA–MON blend, when compared with that for the PEO–MON blend (see Fig. 5). This implies that the crystallinity of PVA is reduced effectively by the well-dispersed MON.

Dynamic Mechanical Properties of Blends

The temperature dependence of the storage (E'), loss (E''), and tan $\delta(E''/E')$ of the blends was investigated; the value of tan δ is a measure of the ratio of energy lost to energy stored per cycle of deformation. Figure 8 shows the DMA curves of the PVA–MON blends. Despite the clay content, E' decreases with increasing temperature and the glass transition can be seen at $\sim 40°C$; the temperature will be referred to as T'_g. Roughly speaking, E' at a given temperature above T'_g increases with increasing ϕ_{mon}. Furthermore, the change in E' at T'_g becomes small with increasing ϕ_{mon}. These results imply that the clay restricts the segmental motions of the PVA amorphous chains. It should be noted that E' values of the PVA15 blends can be measured even at a higher temperature. This result implies that the blend holds its shape even at an elevated temperature. As shown previously, a similar phenomenon can

be observed in the DSC curves; the area of endothermic peaks decreases with increasing ϕ_{mon}. These results suggest that there is a strong interaction between PVA chains and MON. The tan δ versus temperature curves of PVA–MON blends show a maximum at $\sim 50°C$, except for PVA0. The reason for the appearance of the two peaks seen in PVA0 cannot be explained. The lower maximum temperature will be referred to as T_g. Not only the tan δ value at T_g (tan δ_g) but also T_g decreases with increasing ϕ_{mon}, although the change of T_g is small; these results will be discussed later. The PEO–MON blends were so brittle that we cannot perform the DMA measurement of the blends. However, we can obtain the DMA curves of blends of PEO with the organically modified MON (OMON); the preparation for OMON and the PEO–OMON blends can be seen in the previous article.[10] From tan δ versus temperature curves of the PEO–OMON blends, the effects of the OMON
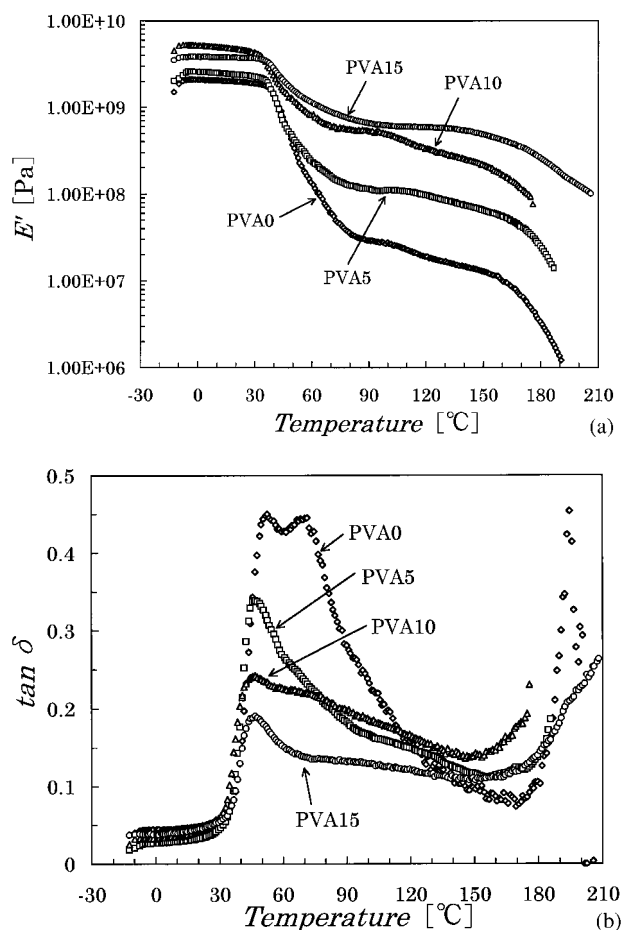

(a)

(b)

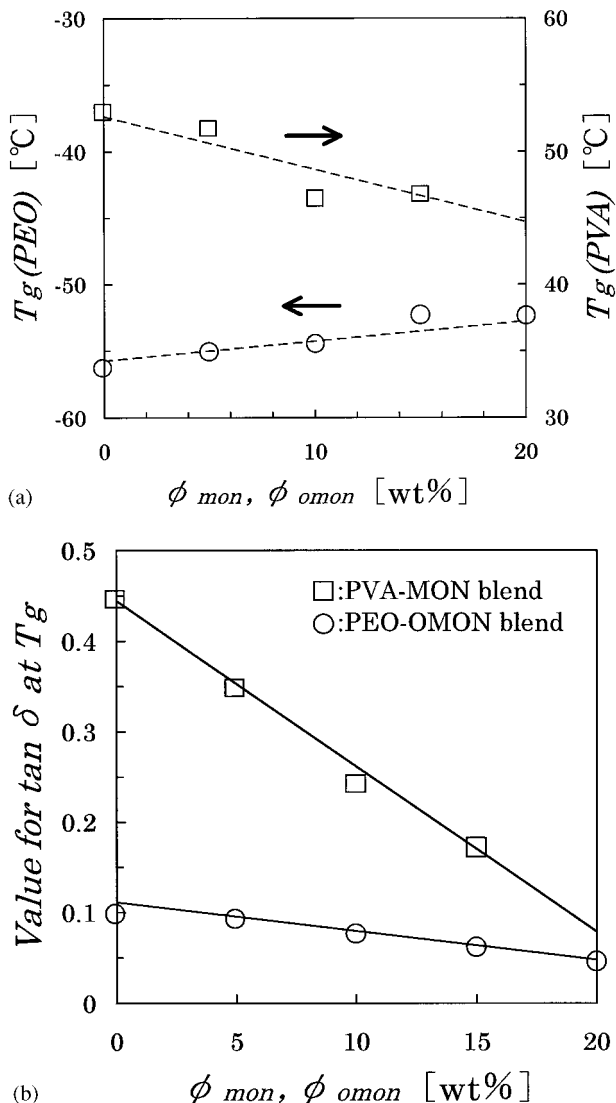**Figure 8**   DMA curves of the PVA–MON blends. (a) E' curves, (b) tan δ curves.

Figure 9   Effects of ϕ_{mon} and ϕ_{omon} on T_g and tan δ_g of PVA–MON and PEO–OMON blends. (a) T_g plots, (b) tan δ_g plots.

content (ϕ_{omon}) on T_g and tan δ_g are also studied. The results are shown in Figure 9, together with those obtained from PVA–MON blends. It is noted that T_g of PVA–MON blends decreases, while that of PEO–OMON blends increases with increasing ϕ_{omon}. This means that the effect of the MON and OMON contents on T_g is not so simple. MON acts as a nucleating agent and the casting temperature is markedly lower than the melting point of PVA. Therefore, its crystallization takes place at a low temperature. Consequently, the residual strains would remain in the amorphous parts of PVA during crystallization. The presence

of unstable amorphous chains may be a reason for the fact that T_g decreases with an increase in ϕ_{mon}. On the other hand, the amorphous chains of PEO would become stable and interact strongly to OMON by the presence of MON during crystallization because the casting temperature is close to the melting point of PEO, and its crystallization takes place at a high temperature. This mechanism may be a reason for T_g decreasing with an increase in ϕ_{omon}. The value of tan δ_g seems to decrease markedly with increasing the clay content in PVA–MON compared with that of PEO–OMON. This suggests that the molecular motion of amorphous chains of PVA is largely restricted by introducing the clay because the silicate layers are well dispersed in this PVA–MON blend.

CONCLUSIONS

Each PEO and PVA is blended with unmodified montmorillonite by using the same solvent, namely water. The structure and mechanical properties of PEO–MON and PVA–MON blends have been investigated. The following conclusions are deduced from the results and discussion.

There is a difference in the clay structure between the two blends: the silicate layers of montmorillonite are well dispersed individually in PVA blends, while the layers form large tactoids in PEO–MON blends. However, the silicate layers in both blends are parallel to the film surface of the blends.

Preferred orientation of PEO and PVA crystallites is induced by the presence of the clay. The chain direction of PVA crystallites is parallel to the silicate layers, while that of PEO is perpendicular to them.

From the measurements of the thermal behavior, it is found that the heat of fusion and the melting point of PEO and PVA decrease with increasing the clay content; the heat of fusion decreases markedly in PVA–MON blends.

The glass transition temperature of PVA decreases slightly, while that of PEO increases with increasing the clay content. The effect of the clay content on molecular motions of polymers is not so simple. The value of tan δ at the glass temperature decreases with increasing the clay content for both blends. However, the decrease is marked in PVA–MON blends.

REFERENCES

1. R. A. Vaia, H. Ishii, and E. P. Giannelis, *Chem. Mater.,* **5,** 1694 (1993).
2. P. B. Messersmith and E. P. Giannelis, *Chem. Mater.,* **6,** 1719 (1994).
3. P. B. Messersmith and E. P. Giannelis, *Chem. Mater.,* **5,** 1064 (1993).
4. P. B. Messersmith and E. P. Giannelis, *J. Polym. Sci., Part A: Polym. Chem.,* **33,** 1047 (1995).
5. A. Usuki, Y. Kojima, M. Kawasumi, A. Okada, Y. Fukushima, T. Kurauchi, and O. Kamigaito, *J. Mater. Res.,* **8,** 1179 (1993).
6. Y. Kojima, A. Usuki, M. Kawasumi, A. Okada, Y. Fukushima, T. Kurauchi, and O. Kamigaito, *J. Mater. Res.,* **8,** 1185 (1993).
7. Y. Kojima, A. Usuki, M. Kawasumi, A. Okada, T. Kurauchi, and O. Kamigaito, *J. Appl. Polym. Sci.,* **49,** 1259 (1993).
8. N. Ogata, G. Jiménez, H. Kawai, and T. Ogihara, *J. Polym. Sci., Part B: Polym. Phys.,* **35,** 389 (1997).
9. G. Jiménez, N. Ogata, and T. Ogihara, *J. Appl. Polym. Sci.,* to appear.
10. N. Ogata, S. Kawakage, and T. Ogihara, *Polymer,* to appear.
11. Y. Fukushima, *Clays and Clay Minerals,* **32,** 320 (1984).
12. F. J. Baltá Calleja and A. Keller, *J. Polym. Sci.: Part A, Polym. Chem.,* **2,** 2127 (1964).
13. C. W. Bunn, *Nature,* **161,** 929 (1948).
14. N. Ogata, T. Ogawa, T. Ida, T. Yanagawa, T. Ogihara, and A. Yamashita, *Sen-i Gakkaishi,* **51,** 439 (1995).